Neuron, Vol. 44, 987–996, December 16, 2004, Copyright ©2004 by Cell Press

Identification of PSD-95 Palmitoylating Enzymes

Masaki Fukata,[1] Yuko Fukata,[1] Hillel Adesnik,[2] Roger A. Nicoll,[2] and David S. Bredt[1,*]
[1]Department of Physiology and
[2]Department of Cellular and Molecular Pharmacology
University of California at San Francisco
San Francisco, California 94143

Summary

Palmitoylation is a lipid modification that plays a critical role in protein trafficking and function throughout the nervous system. Palmitoylation of PSD-95 is essential for its regulation of AMPA receptors and synaptic plasticity. The enzymes that mediate palmitoyl acyl transfer to PSD-95 have not yet been identified; however, proteins containing a DHHC cysteine-rich domain mediate palmitoyl acyl transferase activity in yeast. Here, we isolated 23 mammalian DHHC proteins and found that a subset specifically palmitoylated PSD-95 in vitro and in vivo. These PSD-95 palmitoyl transferases (P-PATs) showed substrate specificity, as they did not all enhance palmitoylation of Lck, SNAP-25b, $G\alpha_s$, or H-Ras in cultured cells. Inhibition of P-PAT activity in neurons reduced palmitoylation and synaptic clustering of PSD-95 and diminished AMPA receptor-mediated neurotransmission. This study suggests that P-PATs regulate synaptic function through PSD-95 palmitoylation.

Introduction

Posttranslational modifications of proteins provide a central molecular mechanism for neurons to respond to external stimuli. The importance of protein phosphorylation cascades in controlling neuronal growth, differentiation, and plasticity is well established. Other protein modifications, including ubiquitination, acetylation, glycosylation, and lipid modification also play crucial roles in neuronal responses to their environment. Lipid modifications not only alter protein structure but also increase the hydrophobicity of proteins, which can cause them to adhere to cellular membranes (Casey, 1994; Dunphy and Linder, 1998; Resh, 1999).

Protein palmitoylation represents a common lipid modification of neuronal proteins (El-Husseini Ael and Bredt, 2002). This posttranslational change involves addition of the saturated 16 carbon palmitate lipid in a thioester linkage to specific cysteine residues. Palmitoylation modifies numerous important neuronal proteins, including the growth-associated protein GAP-43 (Skene and Virag, 1989), G protein α subunits (Degtyarev et al., 1993; Linder et al., 1993; Wedegaertner et al., 1993), nonreceptor tyrosine kinases (Robbins et al., 1995; Shenoy-Scaria et al., 1994), and numerous G protein-coupled receptors (Bouvier et al., 1995). Importantly, palmitoylation occurs in a reversible fashion (Milligan et al., 1995; Mumby, 1997; Ross, 1995; Wedegaertner and Bourne, 1994), which allows palmitoylation to dynamically regulate protein function and to participate in diverse aspects of neuronal signaling.

The postsynaptic density protein, PSD-95, represents a major palmitoylated protein in brain (Topinka and Bredt, 1998). PSD-95 is palmitoylated at cysteine residues 3 and 5 (Topinka and Bredt, 1998). This lipid modification is critical for PSD-95 clustering of AMPA receptors at excitatory synapses (El-Husseini Ael et al., 2002). Furthermore, the palmitoylation of PSD-95 is dynamically regulated by synaptic activity, such that cycling of palmitate on PSD-95 can contribute to aspects of synaptic plasticity (El-Husseini Ael et al., 2002).

Although protein palmitoylation was first identified over 30 years ago, the enzymes that add palmitate to proteins and those that cleave the thioester bond have been elusive. Recent elegant genetic studies in yeast have identified proteins that mediate palmitoyl transferase activity (Linder and Deschenes, 2004; Smotrys and Linder, 2004). Forward genetic screens in yeast identified Erf2/4 (Bartels et al., 1999; Lobo et al., 2002; Zhao et al., 2002) and Akr1p (Roth et al., 2002) as palmitoyl transferases for yeast Ras2 and yeast casein kinase2 (Yck2). Deletion of Erf2/4 or Akr1p prevents palmitoylation of Ras2 or Yck2, respectively. Also, recombinant Erf2/4 and Akr1p palmitoylate Ras2 and Yck2 in vitro; however, these enzymes were inactive toward mammalian proteins. Erf2 and Akr1p share a conserved DHHC cysteine-rich domain (Linder and Deschenes, 2004; Smotrys and Linder, 2004). Our sequence analysis indicates that 23 DHHC proteins are encoded in the human and mouse genomes. Very recently, Keller et al. reported that Golgi apparatus-specific protein with the DHHC zinc finger domain (GODZ; here called DHHC-3), one of the mammalian DHHC proteins, enhanced palmitoyl transfer to GABA-A receptor γ2 subunit in heterologous cells (Keller et al., 2004). However, the biological significance of mammalian DHHC proteins remains unclear.

In this study, we asked whether DHHC proteins function generally as palmitoyl transferases in mammals and whether they could modify PSD-95. We found that four mammalian DHHC proteins can palmitoylate PSD-95 in cultured cells. The DHHC proteins show substrate specificity, as distinct DHHC isoforms preferentially palmitoylate different neuronal proteins. Palmitoylation appears to be direct, as the DHHC proteins can function alone in vitro. Blocking specific palmitoyl transferases reduces palmitoylation and synaptic clustering of PSD-95 and blunts AMPA receptor-mediated synaptic transmission. By palmitoylating PSD-95, specific DHHC proteins control the trafficking of PSD-95 and AMPA receptors, indicating that these enzymes play fundamental roles in controlling synaptic function.

*Correspondence: bredt@itsa.ucsf.edu

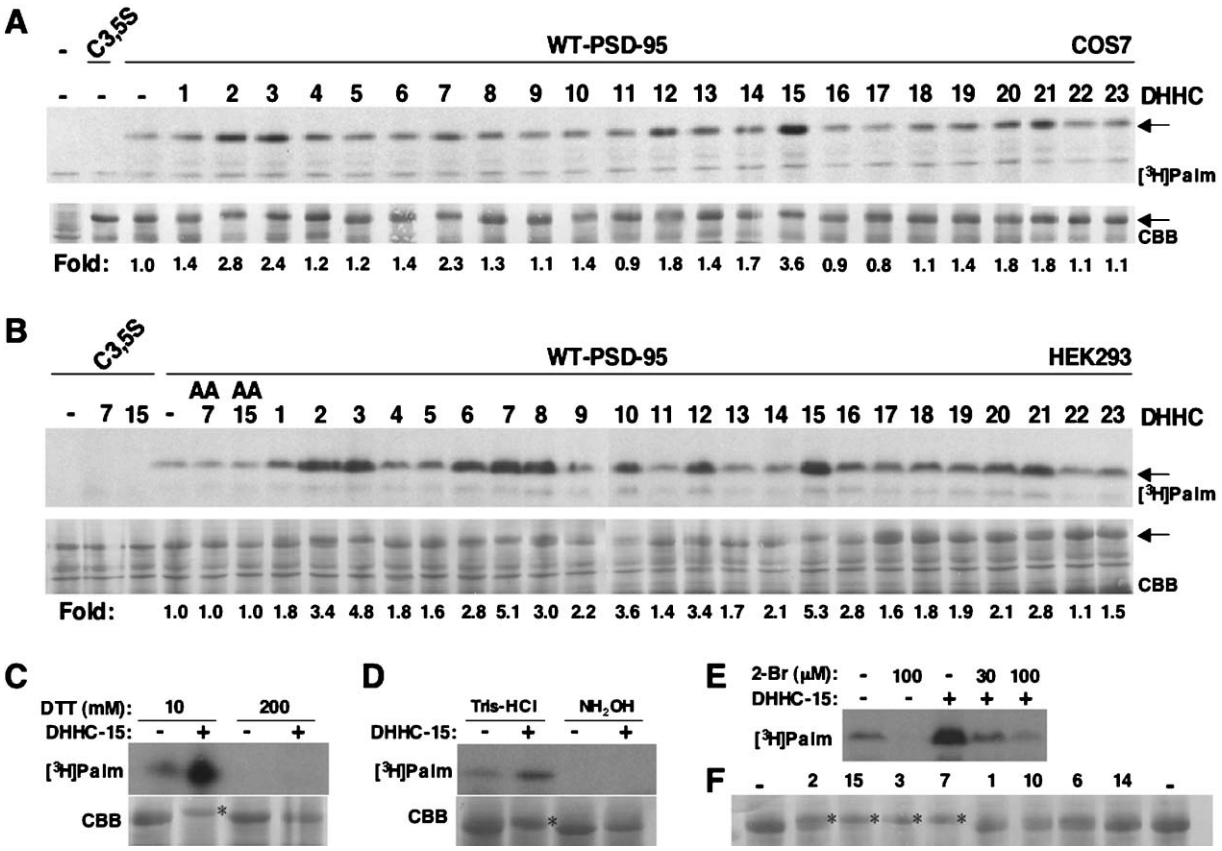

Figure 1. Screening for PSD-95 Palmitoylating Enzymes

(A and B) Individual DHHC clones were transfected together with PSD-95-GFP into COS7 cells (A) and HEK293 cells (B). After metabolic labeling with [^{3}H]palmitate, proteins were separated by SDS-PAGE, followed by fluorography (upper panel; [^{3}H]Palm) and Coomassie brilliant blue staining (lower panel; CBB). Arrows indicate the position of PSD-95-GFP. Enhancement of PSD-95 palmitoylation above control (fold) is indicated beneath each lane. Note that several different DHHC proteins increased incorporation of [^{3}H]palmitate into PSD-95. Mutation of cysteines 3 and 5 of PSD-95 (C3,5S) abolished its palmitoylation. Mutating DH residues in DHHC clones 7 or 15 to AA (AA7, AA15) blocked PSD-95 palmitoylation. Treatment with 200 mM DTT (C) or with 1 M hydroxylamine (NH_2OH) (D) released DHHC-15-mediated [^{3}H]palmitate incorporated into PSD-95 (upper panels). The mobility of palmitoylated PSD-95 by DHHC-15 (indicated by asterisks) is shifted (lower panels). Treatment with DTT or hydroxylamine shifted the mobility of PSD-95 in the presence of DHHC-15 to that of the nonpalmitoylated protein. (E) Treating cells with 2-bromopalmitate (2-Br) blocked the palmitoylation of PSD-95 induced by DHHC-15. (F) Palmitoylation of PSD-95 induces a small shift in migration of PSD-95 as detected by CBB staining. Note that PSD-95 cotransfected with DHHC-2, -3, -7, and -15 but not DHHC-1, -10, -6, or -14 showed mobility shifts (indicated by asterisks).

Results

Identification of PSD-95 Palmitoyl Acyl Transferases

We searched the GenBank database for mouse cDNA clones homologous to the DHHC region of GODZ (DHHC-3), which was identified as a GluR1-interacting protein (Uemura et al., 2002). We isolated and sequenced products from 23 independent mouse genes that encode DHHC proteins (Supplemental Figure S1 [http://www.neuron.org/cgi/content/full/44/6/987/DC1/]). We individually transfected these DNAs together with PSD-95 into COS7 cells (~60% cotransfection) and assessed palmitoylation of PSD-95 by metabolic labeling with [^{3}H]palmitate (Figure 1A). These experiments showed that several different DHHC proteins increased incorporation of [^{3}H]palmitate into PSD-95. The greatest increase was seen with clone 15, which enhanced PSD-95 palmitoylation nearly 4-fold. PSD-95 palmitoylation was increased to >200% of control levels with clones 2, 3, and 7. Mutation of PSD-95 cysteines 3 and 5 to serines abolished palmitoylation. We performed a similar screen in HEK293 cells and found that several clones increased palmitate incorporation into PSD-95 (Figure 1B). Again, the greatest effect was seen with clone 15, which showed about 5.3-fold increase in PSD-95 palmitoylation. Palmitoylation induced by the DHHC proteins in HEK293 cells also required cysteines 3 and 5 of PSD-95. Furthermore, the DHHC motifs were critical, as mutating these residues to alanine in clones 7 or 15 blocked their effects on PSD-95 palmitoylation.

Protein palmitoylation involves acylation of a cysteine to form a labile thioester bond, which is sensitive to reducing agents such as dithiothreitol (DTT) and hydroxylamine (Bizzozero, 1995; Gonzalo and Linder, 1998). Indeed, we found that the [^{3}H]palmitate incorporated into PSD-95 induced by DHHC clone 15 was released by treatment with 200 mM DTT (Figure 1C) or 1 M hydrox-

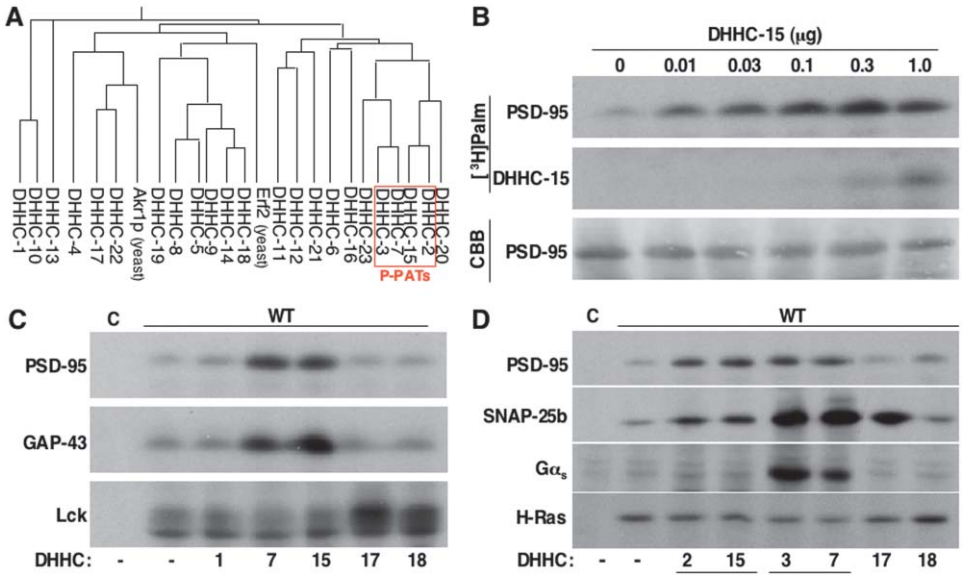

Figure 2. Substrate Specificity of the DHHC Family

(A) The phylogenetic tree shows relative relatedness of P-PATs and other DHHC proteins. (B) Increasing amounts of cotransfected DHHC-15 plasmid palmitoylates PSD-95 (1 μg plasmid) in a dose-dependent manner. Note that DHHC-15 became autopalmitoylated. (C and D) Substrate specificity of DHHC proteins. DHHC clones were transfected together with indicated substrates into HEK293 cells, and palmitoylation was analyzed as in Figure 1. Similar expression level of each substrate was confirmed by immunoblotting (data not shown). The control lane (C) represents PSD-95 (C3, 5S)-GFP; empty vector for GAP-43, Lck, and $G\alpha_s$; SNAP-25b (ΔC), and GFP-H-Ras (C181, 184S).

ylamine (Figure 1D). Previous studies showed that 2-bromopalmitate blocked palmitoylation of PSD-95 in neurons (El-Husseini Ael et al., 2002), and we found that 2-bromopalmitate prevented the palmitoylation of PSD-95 induced by clone 15 (Figure 1E).

We wondered about the stoichiometry of palmitoylation induced by these DHHC proteins. Because the specific activity of [^{3}H]palmitate in cellular metabolic labeling studies is unknown, we could not use this approach to determine the stoichiometry of PSD-95 palmitoylation. However, palmitoylation can shift a protein's apparent molecular weight by SDS-PAGE, and we noted that this shift occurred for the migration of palmitoylated PSD-95 (Figure 1F). That is, we saw a quantitative shift in the mobility of PSD-95 in cells cotransfected with clones 15, 3, and 7. This shift in the mobility of PSD-95 indicates that the protein is quantitatively palmitoylated at at least one, and perhaps both, of the critical cysteines. We saw a partial shift with clone 2; on the other hand, we saw no shift in the mobility of PSD-95 when cotransfected with clones 1, 10, 6, or 14 (Figure 1F). We also found that treatment of palmitoylated PSD-95 by DHHC-15 with 200 mM DTT (Figure 1C) or 1 M hydroxylamine (Figure 1D) shifted it to the position of the nonpalmitoylated PSD-95, indicating that the mobility shift of PSD-95 is due only to palmitoylation.

We noted that the DHHC proteins (encoded by clones 2, 15, 7, and 3) that consistently enhanced PSD-95 palmitoylation in HEK293 and COS7 cells group together on the DHHC phylogenetic tree (Figure 2A). Although DHHC clones 20 and 23 are closely related, they are variable in their activity toward PSD-95 (Figures 1A and 1B). Because four clones (2, 15, 3, and 7) quantitatively induce PSD-95 palmitoylation, we named this group the PSD-95 palmitoyl acyl transferases (P-PATs). The transferase activity appears to be potent and catalytic. That is, DHHC-15 induced PSD-95 palmitoylation even at a 1:100 transfection ratio (Figure 2B). When DHHC-15 was transfected at high levels, it also became palmitoylated (Figure 2B).

Substrate Specificity for P-PATs

Numerous proteins are palmitoylated in neurons and other cells (El-Husseini Ael and Bredt, 2002; Smotrys and Linder, 2004), and we wondered whether DHHC proteins show substrate specificity. We therefore cotransfected the P-PAT cDNAs with other neuronal palmitoylated proteins, including GAP-43 (Skene and Virag, 1989), Lck (Shenoy-Scaria et al., 1994), SNAP-25b (Hess et al., 1992; Lane and Liu, 1997; Vogel and Roche, 1999), G protein α subunits (Degtyarev et al., 1993; Linder et al., 1993; Wedegaertner et al., 1993), and H-Ras (Hancock et al., 1989). We found that DHHC clones showed similar specificity for palmitoylation of GAP-43 and PSD-95 (Figure 2C). On the other hand, Lck was not palmitoylated by P-PATs (DHHC-7 and -15), but rather was palmitoylated by DHHC clones 17 and 18 (Figure 2C). We found that two P-PATs (DHHC-3 and -7) palmitoylated SNAP-25b as did a non-P-PAT (DHHC-17). $G\alpha_s$ showed preference for DHHC-3 and -7. Finally, Ras showed enhanced palmitoylation by DHHC-18, which was otherwise active only toward Lck (Figure 2D). Thus, DHHC-3 and -7 have broad substrate specificity, whereas DHHC-2 and -15 are specific for PSD-95 and GAP-43. We found similar results using COS7 or L cells (data not

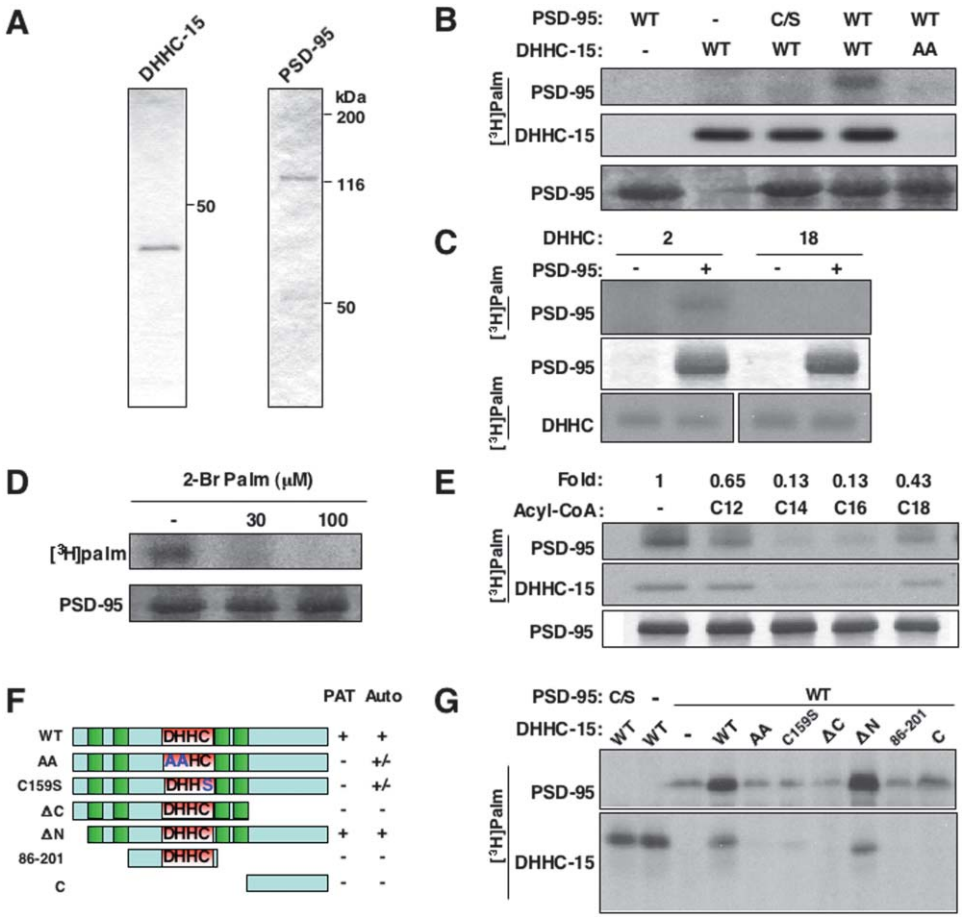

Figure 3. Purified P-PATs Palmitoylate PSD-95 In Vitro

(A) Coomassie staining demonstrates purity of immunoisolated Flag-DHHC-15 and PSD-95-GFP. (B) In vitro palmitoylation. Reactions contained the isolated proteins and [^{3}H]palmitoyl-CoA. Wild-type DHHC-15 palmitoylated wild-type PSD-95 but not PSD-95-C3,5S (C/S). Note that wild-type—but not the DH to AA mutant (AA)—became autopalmitoylated. (C) DHHC-2 but not DHHC-18 palmitoylated PSD-95. (D) DHHC-15-mediated palmitoylation of PSD-95 was blocked in the presence of 2-bromopalmitate (2-Br palm). (E) Fatty acyl-CoA specificity of the DHHC-15. Unlabeled acyl-CoA (2.5 μM each) were added with 0.5 μM [^{3}H]palmitoyl-CoA; lauroyl-CoA (C12), myristoyl-CoA (C14), palmitoyl-CoA (C16), and stearoyl-CoA (C18). Results are expressed as the fraction of PAT activity in the absence of competitor. (F and G) Mutagenesis of DHHC-15 showed that the DHHC core and the C terminus were required for PAT activity. Note that DHHC-15 autopalmitoylation correlated with PSD-95 PAT activity. The signature DHHC motif and transmembrane domains are indicated by red and green boxes, respectively.

shown). Taken together, these experiments show that DHHC proteins show exquisite substrate specificity.

Characterization of P-PAT Activity

We next asked whether a purified P-PAT could palmitoylate purified PSD-95. To address this, we immunoisolated DHHC-15 and PSD-95-GFP. These isolated proteins were homogenous, as determined by Coomassie staining following SDS-PAGE (Figure 3A). Incubation of these purified proteins together with [^{3}H]palmitoyl-CoA showed incorporation of radiolabel into PSD-95 (Figure 3B). This labeling required the critical cysteines at residues 3 and 5 of PSD-95 as well as the conserved DHHC residues of clone 15. Interestingly, only active DHHC-15 autopalmitoylated. As a control, we found that DHHC clone 18, which showed autopalmitoylation activity, was inactive toward PSD-95, whereas DHHC-2, another P-PAT, palmitoylated purified PSD-95 (Figure 3C). This in vitro palmitoyl transferase activity was also blocked by 2-bromopalmitate (Figure 3D).

The lipid substrate specificity of DHHC-15 was examined by adding unlabeled acyl-CoA competitors (at 2.5 μM, a 5-fold excess) to the radioactive in vitro PAT reaction. Addition of myristoyl-CoA (C14) and palmitoyl-CoA (C16) resulted in >80% inhibition (Figure 3E). Lauroyl-CoA (C12) and stearoyl-CoA (C18) were less effective at similar concentrations (~35% and ~55% inhibition, respectively). This lack of strict acyl-CoA substrate specificity for P-PAT correlates with the heterogeneity of thioester-linked fatty acids on proteins in vivo (Smotrys and Linder, 2004).

To identify the critical domains for P-PAT activity, mutants of DHHC-15 were constructed and transfected into HEK293 cells, and palmitoylation of PSD-95 was assessed by [^{3}H]palmitate metabolic labeling (Figures 3F and 3G). DHHC-15 (wt) and -ΔN (aa 19–337) enhanced PSD-95 palmitoylation. We found that AAHC-15, DHHC-15-ΔC (aa 1–238), (aa 86–201) and -C (aa 239–337) did not enhance PSD-95 palmitoylation. Another mutant in the core domain (DHHC-15-C159S) also failed to en-

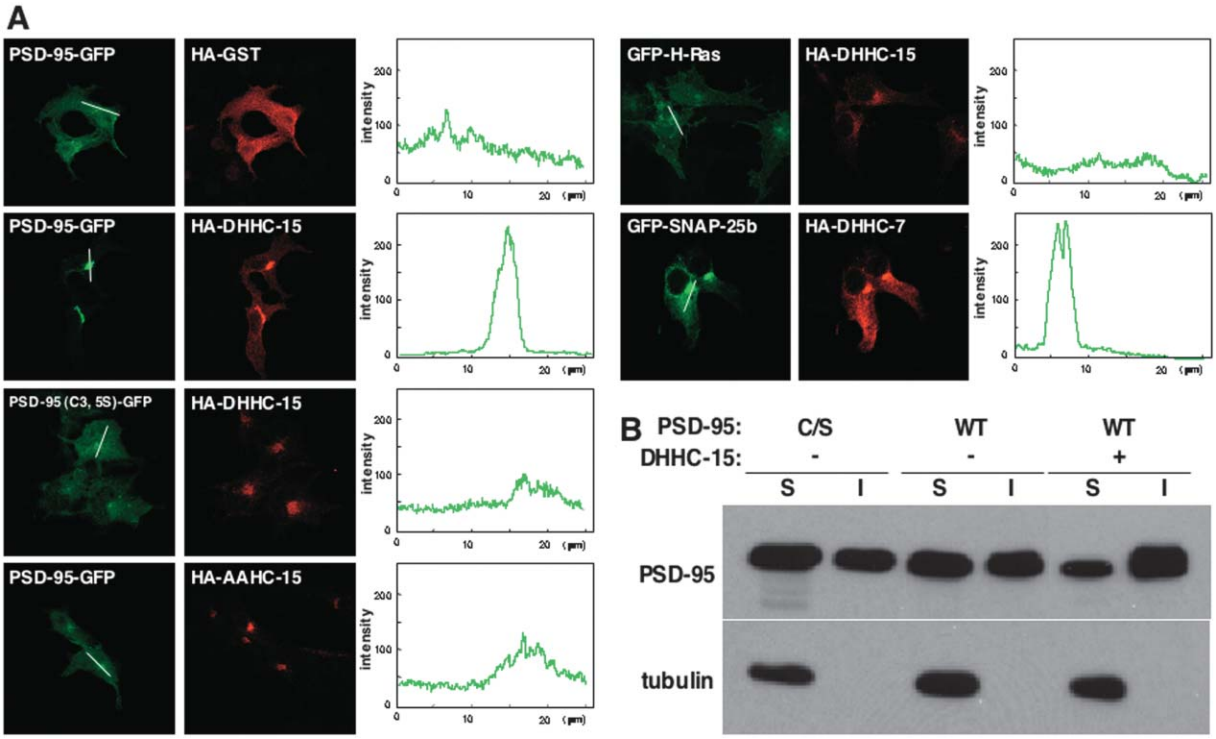

Figure 4. Effect of DHHC Protein on PSD-95 Distribution in HEK293 Cells

(A) Indicated GFP-tagged cDNAs (PSD-95, H-Ras, and SNAP-25b) were cotransfected with HA-tagged DHHC clones into HEK293 cells. The cells were stained by anti-HA antibody (red). The GFP fluorescence intensity (green) on the white lines (25 μm) was calculated by the LSM510 software and quantitated graphically. DHHC-15 specifically increased the segregation of wild-type PSD-95—but not H-Ras—to the perinuclear region. Mutating the DH residues to AA (AAHC-15) blocked the effect of DHHC-15 on PSD-95 trafficking. Cotransfection of DHHC-7 with SNAP-25b caused redistribution of SNAP-25b to a perinuclear domain. (B) DHHC-15 redistributes PSD-95 from Triton X-100-soluble to -insoluble fractions. Triton X-100-soluble (S) and -insoluble (I) fractions from transfected HEK293 cells were separated and probed for PSD-95 and tubulin.

hance PSD-95 palmitoylation, consistent with the previous report in yeast Akr1p (Roth et al., 2002) (Figures 3F and 3G). The PAT activity of DHHC-15 correlated with its autopalmitoylation (Figures 3F and 3G).

P-PAT Activity Targets PSD-95 to Cellular Membranes

We next asked whether P-PATs could modulate the function of PSD-95 in vivo. Previous studies showed that palmitoylation targets PSD-95 to a perinuclear domain (El-Husseini et al., 2000a). Fitting with this, we found that cotransfection with clone 15 increased the segregation of PSD-95 to this perinuclear region (Figure 4A). This redistribution required the critical cysteines of PSD-95 and also the DHHC region of clone 15. This effect was specific, as clone 15 did not alter the distribution of H-Ras (Figure 4A). Furthermore, DHHC-7, which palmitoylates SNAP-25b (Figure 2D), increased the targeting of SNAP-25b to the perinuclear region. This redistribution required the critical cysteines of SNAP-25b (data not shown). We found that this redistribution of PSD-95 and SNAP-25b was likely not due to their physical interaction with DHHC proteins, because we could not detect stable association by immunoprecipitation (data not shown). However, we cannot neglect the possibility that direct binding contributes to redistribution of PSD-95 as reported for GODZ (DHHC-3) and GABA-A receptor γ2 subunit (Keller et al., 2004).

Our previous work showed that palmitoylation regulates the association of PSD-95 with cellular membranes (El-Husseini Ael et al., 2002; Topinka and Bredt, 1998). In transfected HEK293 cells, PSD-95 fractionates with both the Triton X-100-soluble and Triton X-100-insoluble (membrane-associated) fractions. This heterogeneous fractionation held true for both wild-type PSD-95 as well as the mutant lacking the critical cysteines at positions 3 and 5. Cotransfection with clone 15 caused redistribution of wild-type PSD-95 to the membrane-associated fraction (Figure 4B). This effect was specific, as clone 15 did not alter the fractionation of tubulin.

P-PATs Regulate PSD-95 Function in Neurons

Next, we asked if P-PATs are expressed in brain. Previous reports showed that DHHC-2 (ream) (Oyama et al., 2000) and DHHC-3 (GODZ) (Uemura et al., 2002) are expressed ubiquitously in brain and peripheral tissues. Our Northern blotting experiments showed that the 3.1 kb DHHC-7 mRNA was also widely expressed in brain and peripheral tissues; by contrast, the 5.8 kb DHHC-15 mRNA was expressed mainly, but not exclusively, in brain (Figure 5A). We found that DHHC-18 mRNA, which has PAT activity for H-Ras, was expressed ubiquitously

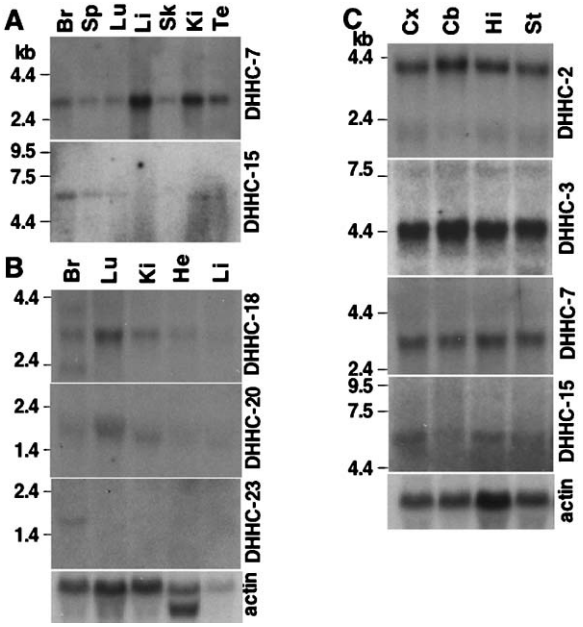

Figure 5. P-PATs Are Expressed in Brain

Northern blot analysis used mRNA (2 μg) (A) or total RNA (20 μg) (B and C) isolated from different mouse tissues (A and B) and brain regions (C). Br, brain; Sp, spleen; Lu, lung; Li, liver; Sk, skeletal muscle; Ki, kidney; Te, testis; He, heart; Cx, cortex; Cb, cerebellum; Hi, hippocampus; St, striatum.

and DHHC-20, closely related to DHHC-2 and 15, occurred mainly in lung (Figure 5B). DHHC-23, closely related to DHHC-3 and -7, was largely restricted to brain (Figure 5B). DHHC-17 (HIP14), which has PAT activity for SNAP-25b, was expressed widely (Singaraja et al., 2002). All four P-PATs were expressed in all brain regions, including cerebral cortex, cerebellum, hippocampus, and striatum (Figure 5C).

To determine whether P-PATs palmitoylate endogenous PSD-95, we sought to identify a dominant-negative P-PAT construct. When cotransfected with wild-type DHHC-15, the AAHC-15 or C159S mutant blocked PSD-95 palmitoylation (Figure 6A). C159S mutant also blocked DHHC-2-induced, but not DHHC-3- or -7-induced, PSD-95 palmitoylation. Furthermore, C159S did not affect DHHC-3-induced GAP-43 palmitoylation or DHHC-3-induced $G\alpha_s$ palmitoylation (Supplemental Figure S2 [http://www.neuron.org/cgi/content/full/44/6/987/DC1/]). Under these conditions, other mutants with no PAT activity, such as DHHC-15-ΔC and DHHC-15-C, failed to inhibit PAT activity of DHHC-15 (data not shown). Consistent with these data, C159S inhibited DHHC-15-induced, but not DHHC-3-induced, PSD-95 redistribution to perinuclear regions (Figure 6B).

We used these tools to study endogenous PSD-95 palmitoylation in neurons. Metabolic labeling experiments showed that GFP-DHHC-15 quadrupled PSD-95 palmitoylation (Figure 6C), whereas GFP-C159S inhibited neuronal PSD-95 palmitoylation (57.6% ± 4.0% of control cells, $n = 4$, $^*p < 0.001$) (Figure 6C). Next, we asked whether P-PATs control PSD-95 synaptic clustering and function. Overexpression of GFP-DHHC-15 in neurons increased the amount of PSD-95 in Triton X-100-insoluble fractions (Figure 7A). In contrast, inhibition of P-PAT activity by GFP-C159S increased the amount of soluble PSD-95 (Figure 7A). Under these conditions, the subcellular distribution of other palmitoylated proteins, $G\alpha_s$ and Lck, did not change. Expression of the dominant-negative C159S mutant significantly inhibited PSD-95 synaptic clustering, whereas wild-type DHHC-15 did not (Figure 7B). Because PSD-95 palmitoylation controls AMPA receptor function (El-Husseini et al., 2000b; El-Husseini Ael et al., 2002), we examined clustering of AMPA receptor subunit GluR2. Expression of C159S significantly reduced surface clustering of GluR2, whereas wild-type DHHC did not (Figure 7B). Under the conditions, the clustering of synaptophysin (Figure 7B) and the NR1 subunit of NMDA receptors (data not shown) did not change. Finally, we asked whether inhibition of P-PAT activity by C159S changed glutamatergic transmission. AMPA receptor-mediated miniature excitatory postsynaptic currents (mEPSCs) were monitored with whole-cell recordings from cultured hippocampal neurons. We found a significant reduction in the amplitude of synaptic events in C159S-infected neurons (Figure 7Cb), but not in DHHC-15-infected cells (Figure 7Ca).

Discussion

This study identifies a family of four P-PAT enzymes that are expressed in brain and can mediate palmitoyl transfer to PSD-95. These enzymes share a conserved and critical DHHC motif, which has been found in palmitoyl transferases in yeast (Lobo et al., 2002; Roth et al., 2002). The enzymes can function alone in vitro and show specificity for neuronal substrate proteins. Furthermore, P-PATs regulated AMPA receptor-mediated synaptic function through PSD-95 palmitoylation.

Understanding the catalytic mechanism for P-PATs represents an important future goal. The thioester bond in the substrate palmitoyl-CoA is of high energy and is similar to that in the palmitoylated protein product. This indicates that an energy source is not necessary for this reaction. Indeed, we find that a purified P-PAT can directly modify purified PSD-95. It is interesting to note that P-PATs, as well as the other DHHC proteins (Lobo et al., 2002; Roth et al., 2002), autoacylate in the presence of palmitoyl-CoA, and this requires the signature DHHC domain. This may indicate that a thioester intermediate on the DHHC protein underlies the reaction mechanism.

Mechanisms that control the activity of P-PATs remain uncertain. Previous work shows that palmitate turnover on proteins can be dynamically regulated by physiological stimuli. Palmitate turnover on $G\alpha$ subunits is rapidly increased by activation of their associated G protein-coupled receptors (Wedegaertner and Bourne, 1994). Furthermore, palmitate cycling on PSD-95 is augmented by calcium influx through NMDA receptors, which are also linked to PSD-95 (El-Husseini Ael et al., 2002). In yeast, the DHHC protein Akr1p palmitoylates casein kinase, and this activity is increased by ATP in vitro (Roth et al., 2002). It will be critical to determine whether nucleotides or other second messengers might control the activity of P-PATs in neurons. In our previous paper (El-

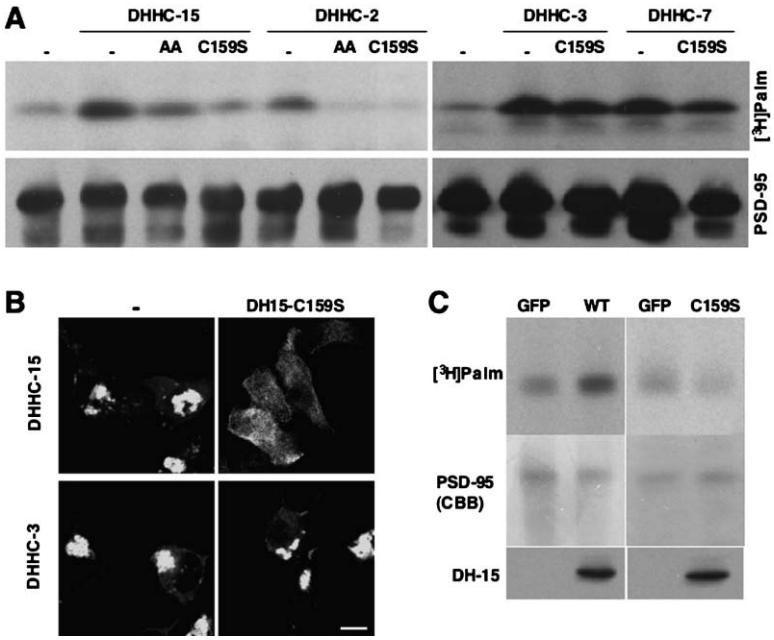

Figure 6. P-PATs Participate in PSD-95 Palmitoylation in Neurons

(A) Mock vector (indicated by "−"), AAHC-15 (AA), or C159S mutant (see Figure 3F) were cotransfected with DHHC clones 15, 2, 3, or 7 together with PSD-95 into HEK293 cells. After metabolic labeling with [^{3}H]palmitate, proteins were separated by SDS-PAGE, visualized by fluorography (upper panel; [^{3}H]Palm) and immunoblotted with anti-PSD-95 (lower panel). C159S (and to a lesser extent AA) inhibited DHHC-15- or -2-induced, but not DHHC-3- or -7-induced, PSD-95 palmitoylation. (B) C159S together with DHHC-15 or DHHC-3 were cotransfected with PSD-95-GFP into HEK293 cells. C159S blocked DHHC-15- but not DHHC-3-induced PSD-95 redistribution to perinuclear regions. Scale bar, 10 μm. (C) Cultured hippocampal neurons were infected with Semliki forest viruses expressing GFP, GFP-DHHC-15 wild-type (wt), or GFP-C159S. The neurons were treated with 3 mCi/ml [^{3}H]palmitate for 4 hr. Immunoprecipitated PSD-95 was resolved by SDS-PAGE, followed by fluorography ([^{3}H]Palm) and Coomassie staining (CBB). Wild-type DHHC-15 enhanced whereas the C159S mutant inhibited palmitoylation of PSD-95.

Husseini Ael et al., 2002), we suggested that unidentified palmitoyl thioesterase enzymes control activity-stimulated palmitate turnover on PSD-95. Whether P-PAT activity might also be regulated by neuronal activity will require future studies.

Members of the large family of 23 mammalian DHHC proteins have a conserved region that includes the catalytically critical DHHC domain. However, the C-terminal and N-terminal regions of these proteins are divergent and some contain regulatory regions such as SH3 domains or ankyrin repeats. This is akin to protein kinases, which also share a core catalytic region and differ in regulatory domains that afford for differential control.

It is interesting that the P-PATs occur on one limb of the DHHC phylogenetic tree (Figure 2A), and this may reflect a structural correlate to enzyme specificity for PSD-95 palmitoylation. The cysteines of palmitoylated PSD-95 occur near the N terminus; however, a diversity of other sequences in other proteins can be palmitoylated. Transmembrane proteins often are palmitoylated at juxtamembrane locations. Palmitoylation can also occur in the context of other lipid modifications (El-Husseini Ael and Bredt, 2002; Smotrys and Linder, 2004). Ras protein is palmitoylated at a C-terminal site that is adjacent to a site for prenylation; $G\alpha_i$ subunit is palmitoylated at an N-terminal cysteine that is adjacent to sites for myristoylation. In light of the results here, we suspect that other limbs of the DHHC phylogenetic tree will show specificity for these other classes of palmitoylated proteins.

The family of DHHC palmitoyl transferases represent intriguing drug targets. The transforming activity of oncogenes require their palmitoylation (Hancock et al., 1989). In the nervous system, numerous synaptic proteins, including serotonin receptors and synaptic vesicle proteins, are palmitoylated (El-Husseini Ael and Bredt, 2002). The specificity of the DHHC enzymes for protein substrates suggests that therapeutically useful antagonists may exist with defined sites of action. It will be important to develop these isoform-specific modulators of P-PATs and other DHHC enzymes to determine the physiological and pathological roles for these enzymes throughout the body.

Experimental Procedures

Cloning and Plasmid Constructions

cDNAs encoding mouse DHHC proteins and mouse H-Ras were cloned by RT-PCR using mouse brain total RNA or amplified from isolated EST clones (for clone 10, 13, and 19) and primers (see Supplemental Figure S1 [http://www.neuron.org/cgi/content/full/44/6/987/DC1/]). All PCR products were analyzed by DNA sequencing. The cDNAs were subcloned into pEF-Bos-HA, pEGFP-C1 (BD Biosciences), pCAGGS-FLAG, and pSCA1 (Stein et al., 2003). To obtain DHHC-15-ΔC (aa 1–238), -ΔN (aa 19–337), (aa 86–201), and -C (aa 239–337), the corresponding fragments were subcloned into pEF-Bos-HA. The mutants AA-7, AA-15, and C159S were generated using a site-directed mutagenesis by changing DH (aa 157 and 158; DHHC-7) to AA, DH (aa 156 and 157; DHHC-15) to AA, and C (aa 159; DHHC-15) to S, respectively. EGFP-C1-H-Ras (C181, 184S) was also generated with a site-directed mutagenesis. pGW1-PSD-95, PSD-95 (C3, 5S), and GAP-43 fused to GFP were described previously (El-Husseini et al., 2000a). pcDNA3-SNAP-25b and pcDNA3-SNAP-25b (ΔC), whose palmitoylated cysteines were deleted, were provided by Dr. Paul A. Roche (National Institutes of Health, MD) (Vogel and Roche, 1999). pcDNA3-HA-$G\alpha_s$ was a gift of Dr. Philip B. Wedegaertner (Thomas Jefferson University, PA) (Evanko et al., 2000). The Lck cDNA was provided by Dr. Art Weiss (UCSF) and was subcloned into pcDNA3.1.

In Vivo Palmitate Labeling

Transfected HEK293 or COS7 cells were preincubated for 30 min in serum-free DMEM with fatty acid-free bovine serum albumin (10 mg/ml; Sigma). Cells were then labeled with 0.5 mCi/ml [^{3}H]palmitic acid (PerkinElmer) for 4 hr in the preincubation medium. Cells were washed with PBS, scraped with SDS-PAGE sample buffer (62.5 mM Tris-HCl [pH 6.8], 10% glycerol, 2% SDS, and 0.001% bromophenol blue) with 10 mM DTT and boiled for 2 min. For DTT treatment, radiolabeled proteins were dissolved in SDS sample buffer with 200

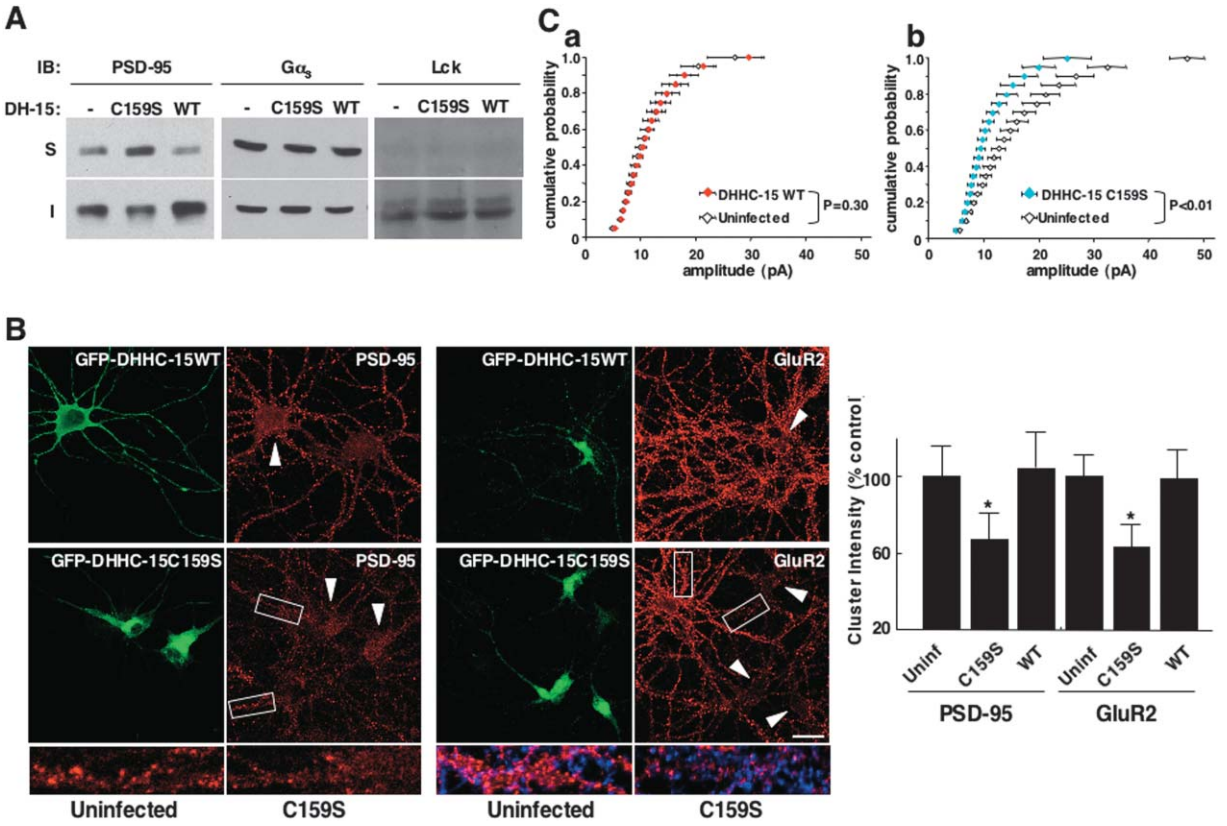

Figure 7. Inhibition of P-PATs Perturbs PSD-95 Function in Neurons

(A) Cultured hippocampal neurons infected with Semliki forest virus expressing GFP (indicated as "−"), GFP-DHHC-15 (wt), or GFP-C159S were harvested, and the lysates were fractionated. Triton X-100-soluble (S) and -insoluble (I) fractions were separated and probed for PSD-95, $G\alpha_s$, and Lck. (B) Cultured hippocampal neurons were infected with Semliki forest virus expressing GFP-DHHC-15 (wt) or GFP-C159S. At 24 hr after infection, PSD-95 and surface GluR2 were stained (red). Infected neurons are indicated by arrowheads. Higher-magnification micrographs of the boxed regions are shown in the panels below. Synaptophysin (blue) and GluR2 (red) were doubly stained. Quantitative analysis shows that C159S reduced synaptic PSD-95 and surface GluR2 clustering (*$p < 0.001$). Scale bar, 10 μm. (C) Overexpression of GFP-C159S (b) ($n = 6$), but not DHHC-15 (a) ($n = 7$), significantly (Student's t test) reduced the amplitude of AMPA receptor-mediated mEPSCs.

mM DTT and boiled for 5 min (Bizzozero, 1995). For $G\alpha_s$ palmitate labeling, the cells were treated with 10% (w/v) trichloroacetic acid. The resulting precipitates were suspended in SDS sample buffer with 10 mM DTT. For fluorography, protein samples were separated by SDS-PAGE. Gels were treated with Amplify (Amersham) for 30 min, dried under vacuum, and exposed to (Kodak Biomax MS) at −80°C. After autoradiography, the bands were scanned and analyzed with NIH software. To quantitate the relative PAT activity of each DHHC clone, we quantitated the ratio of palmitoylated PSD-95 to total PSD-95 (measured by Coomassie staining). For hydroxylamine treatment, radiolabeled cells were sonicated in phosphate buffer and suspended with 1 M hydroxylamine (NH_2OH) (pH 7.0) or 1 M Tris-HCl (pH 7.0). For 2-bromopalmitate treatment, HEK293 cells were labeled with [^{3}H]palmitic acid in the presence of 2-bromopalmitate.

Cultured hippocampal neurons (5×10^5 cells/well) (DIV 16–21) were infected with GFP-DHHC-15 wild-type or C159S expressing Semliki forest virus (Stein et al., 2003). At 20 hr after infection, the cells were labeled for 4 hr in neurobasal media containing 3 mCi/ml [^{3}H]palmitic acid. Labeled cells were washed with PBS and resuspended in 0.15 ml lysis buffer A (20 mM Tris-HCl [pH 7.4], 1 mM EDTA, 100 mM NaCl, and 1% SDS). After 5 min extraction, 1% Triton X-100 was added to a final volume of 1.5 ml. After centrifugation at 20,000 × g for 10 min, the supernatants were incubated with rabbit anti-PSD-95 antibody (El-Husseini Ael et al., 2002) for 1 hr and then incubated for 1 hr with 30 μl protein A Sepharose (Pharmacia) at 4°C. Immunoprecipitates were washed three times with buffer containing 20 mM Tris-HCl (pH 7.4), 1 mM EDTA, 100 mM NaCl, and 1% Triton X-100. Immunoprecipitated PSD-95 was resolved by SDS-PAGE, followed by fluorography and Coomassie staining.

Preparation of Recombinant Proteins

FLAG-tagged DHHC clones were purified from transfected HEK293 cells seeded onto a 10 cm dish (5×10^6 cells). At 24 hr after transfection, cells were lysed with lysis buffer B (20 mM Tris-HCl [pH 7.4], 1 mM EDTA, 100 mM NaCl, 1% Triton X-100, 10 μg/ml leupeptin). The lysates were mixed with 25 μl anti-FLAG M2 mAb-Agarose (Sigma) for 2 hr at 4°C. After washing the beads with buffer C (20 mM Tris-HCl [pH 7.4], 1 mM EDTA, 50 mM NaCl, 0.1% Triton X-100, 10 μg/ml leupeptin), the bound proteins were eluted by addition of buffer D (20 mM Tris-HCl [pH7.4], 0.05% Triton X-100, 250 μg/ml FLAG peptide). PSD-95-GFP was immunoprecipitated by anti-GFP antibody from transfected HEK293 cells. After washing the beads with buffer C, the beads were taken up in buffer E (20 mM Tris-HCl [pH7.4], 0.05% Triton X-100).

In Vitro PAT Assay

[^{3}H]palmitoyl-CoA was synthesized from [^{3}H]palmitic acid and CoA using acyl-CoA synthetase (Sigma) and purified as described (Taylor et al., 1990). The PAT assay was performed as described (Lobo et al., 2002; Roth et al., 2002). Briefly, FLAG-DHHC (50 nM) was added to PSD-95-GFP beads (100 nM) in 50 mM MES (pH 6.4). The reaction was started by the addition of 0.5 μM [^{3}H]palmitoyl-CoA (0.5 μCi), incubated for 1 hr at 30°C and stopped by the addition of a 2× SDS sample buffer with 20 mM DTT. Reaction proteins were resolved by SDS-PAGE, followed by fluorography and silver staining.

Immunofluorescence Analysis

HEK293 cells were seeded onto three 12 mm cover slips in each well of a 6-well cell culture plate (3×10^5 cells/well). At 24 hr after transfection, the cells were fixed with 4% paraformaldehyde at room temperature for 10 min, permeabilized with 0.1% Triton X-100 for 10 min, and blocked with PBS containing 2 mg/ml bovine serum albumin for 10 min on ice. The fixed cells were stained with anti-HA mouse monoclonal antibody (Covans) and Cy3-conjugated secondary antibody. Hippocampal neurons (DIV 14–21; 0.5×10^5) were seeded onto 12 mm coverslips. The neurons were infected with GFP-DHHC-15 wild-type or C159S expressing Semliki forest virus. At 24 hr after infection, the neurons were fixed as above and stained with anti-PSD-95 mouse monoclonal antibody (Affinity Bio Reagents), followed by Cy3-conjugated secondary antibody. For surface GluR2 staining, surface GluR2 receptors were "live"-labeled with an antibody to an extracellular epitope of GluR2 (Chemicon) by incubating neurons in conditioned medium for 15 min at 37°C. Neurons were fixed with 4% paraformaldehyde/120 mM sucrose/100 mM HEPES (pH 7.4) on ice for 10 min and blocked with PBS containing 2 mg/ml bovine serum albumin for 10 min on ice. Surface GluR2 was visualized with Cy3-conjugated secondary antibody. Subsequently, neurons were permeabilized with 0.1% Triton X-100 for 10 min and stained with anti-synaptophysin rabbit polyclonal antibody (Zymed) and Cy5-conjugated secondary antibody. Fluorescent images were taken with a confocal laser microscopy system (Carl Zeiss LSM 510; Carl Zeiss, Oberkochen, Germany). The intensity of the fluorescence was calculated using LSM510 software. To quantitate changes in clustering, ten fields were chosen from three independent neuronal cultures, and the three largest caliber proximal dendrites ($\sim$20 μm long) were analyzed (at least 300 clusters). Synaptic clustering was defined as sites containing PSD-95 or synaptophysin at intensities at least twice the dendritic background. We measured the maximum intensities of all synaptic clusters along these dendritic segments in infected and neighboring noninfected cells and analyzed data by Student's t test. An experimenter blind with regard to virus treatment stained and measured protein clustering.

Subcellular Fractionation

HEK293 cells were seeded onto 6-well plate (5×10^5 cells/well). At 24 hr after transfection, the cells were suspended with lysis buffer B. Lysates were centrifuged at 20,000 $\times$ g for 10 min at 4°C. The supernatants were collected and pellets were resuspended in SDS sample buffer. Fractions (supernatant:pellet = 1:1) were resolved by SDS-PAGE and immunoblotted for PSD-95 (El-Husseini Ael et al., 2002) and tubulin (SIGMA). Cultured hippocampal neurons (DIV 14–21; 0.5×10^5) were infected with Semliki forest virus. At 24 hr after infection, cells were washed with PBS, harvested, and then suspended with lysis buffer B. Lysates were centrifuged at 20,000 $\times$ g for 10 min at 4°C. The supernatants were collected and pellets were resuspended in SDS sample buffer. Fractions (supernatant:pellet = 1:1) were resolved by SDS-PAGE and immunoblotting for PSD-95, $G\alpha_s$ (Upstate), and Lck (Chemicon).

Northern Blot

Total RNA was isolated from mouse tissue using the TRIzol reagent (Invitrogen), and mRNA was isolated with oligodT columns. Twenty micrograms of total RNA or 2 μg mRNA were separated on a formaldehyde agarose gel and transferred to a nylon membrane. The membranes were hybridized with random primed [α-^{32}P]dCTP DHHC cDNA probes; DHHC-2, nucleotides 602–1101; DHHC-3, nucleotides 381–900; DHHC-7, nucleotides 429–927; DHHC-15, nucleotides 1–1014; DHHC-18, nucleotides 1–759; DHHC-20, nucleotides 1–1104; DHHC-23, nucleotides 1–837. The blots were also hybridized with a β-actin cDNA probe.

Patch Clamp Recording

Recordings were performed at room temperature with an Axopatch-1B amplifier and patch pipettes of 3–5 MΩ. Series resistances ranged between 10 and 20 MΩ. The external solutions contained 140 mM NaCl, 2.4 mM KCl, 10 mM HEPES, 10 mM glucose, 4 mM $CaCl_2$, 4 mM $MgCl_2$, 0.1 mM picrotoxin, and 0.005 mM TTX (pH 7.27). The internal solution contained 107.5 mM d-gluconic acid, 20 mM HEPES, 0.2 mM EGTA, 8 mM NaCl, 10 mM TEA-Cl, 4 mM Mg-ATP, 0.3 mM Mg-GTP, 5 mM QX-314, and 0.1 mM spermine (pH 7.2). mEPSCs (about 100 events per cell) were automatically detected using in-house software. Picrotoxin and TTX were from Sigma.

Acknowledgments

We thank Drs. Alexander Alexendrov, Lars Funke, Maki Takamoto, and Robert Edwards for helpful suggestions and discussion; Dr. Akihiko Kato for helping with the hippocampal cell culture; and Dr. Kaiwen Kam for writing the mEPSC analysis software. M.F. is supported by Japan Society for the Promotion of Science. Y.F. is supported by long-term fellowship of The International Human Frontier Science Program Organization. H.A. is supported by a Howard Hughes predoctoral fellowship. R.A.N. is a member of the Keck Center for Integrative Neuroscience and the Silvio Conte Center for Neuroscience Research. D.S.B. is supported by grants from the National Institutes of Health, Christopher Reeves Paralysis Foundation, Human Frontier Science Program, and American Heart Association.

Received: June 24, 2004
Revised: October 4, 2004
Accepted: November 23, 2004
Published: December 15, 2004

References

Bartels, D.J., Mitchell, D.A., Dong, X., and Deschenes, R.J. (1999). Erf2, a novel gene product that affects the localization and palmitoylation of Ras2 in Saccharomyces cerevisiae. Mol. Cell. Biol. *19*, 6775–6787.

Bizzozero, O.A. (1995). Chemical analysis of acylation sites and species. Methods Enzymol. *250*, 361–379.

Bouvier, M., Loisel, T.P., and Hebert, T. (1995). Dynamic regulation of G-protein coupled receptor palmitoylation: potential role in receptor function. Biochem. Soc. Trans. *23*, 577–581.

Casey, P.J. (1994). Lipid modifications of G proteins. Curr. Opin. Cell Biol. *6*, 219–225.

Degtyarev, M.Y., Spiegel, A.M., and Jones, T.L. (1993). Increased palmitoylation of the Gs protein alpha subunit after activation by the beta-adrenergic receptor or cholera toxin. J. Biol. Chem. *268*, 23769–23772.

Dunphy, J.T., and Linder, M.E. (1998). Signalling functions of protein palmitoylation. Biochim. Biophys. Acta *1436*, 245–261.

El-Husseini, A.E., Craven, S.E., Chetkovich, D.M., Firestein, B.L., Schnell, E., Aoki, C., and Bredt, D.S. (2000a). Dual palmitoylation of PSD-95 mediates its vesiculotubular sorting, postsynaptic targeting, and ion channel clustering. J. Cell Biol. *148*, 159–171.

El-Husseini, A.E., Schnell, E., Chetkovich, D.M., Nicoll, R.A., and Bredt, D.S. (2000b). PSD-95 involvement in maturation of excitatory synapses. Science *290*, 1364–1368.

El-Husseini Ael, D., and Bredt, D.S. (2002). Protein palmitoylation: a regulator of neuronal development and function. Nat. Rev. Neurosci. *3*, 791–802.

El-Husseini Ael, D., Schnell, E., Dakoji, S., Sweeney, N., Zhou, Q., Prange, O., Gauthier-Campbell, C., Aguilera-Moreno, A., Nicoll, R.A., and Bredt, D.S. (2002). Synaptic strength regulated by palmitate cycling on PSD-95. Cell *108*, 849–863.

Evanko, D.S., Thiyagarajan, M.M., and Wedegaertner, P.B. (2000). Interaction with Gbetagamma is required for membrane targeting and palmitoylation of Galpha(s) and Galpha(q). J. Biol. Chem. *275*, 1327–1336.

Gonzalo, S., and Linder, M.E. (1998). SNAP-25 palmitoylation and plasma membrane targeting require a functional secretory pathway. Mol. Biol. Cell *9*, 585–597.

Hancock, J.F., Magee, A.I., Childs, J.E., and Marshall, C.J. (1989). All ras proteins are polyisoprenylated but only some are palmitoylated. Cell *57*, 1167–1177.

Hess, D.T., Slater, T.M., Wilson, M.C., and Skene, J.H. (1992). The

25 kDa synaptosomal-associated protein SNAP-25 is the major methionine-rich polypeptide in rapid axonal transport and a major substrate for palmitoylation in adult CNS. J. Neurosci. *12*, 4634–4641.

Keller, C.A., Yuan, X., Panzanelli, P., Martin, M.L., Alldred, M., Sassoe-Pognetto, M., and Luscher, B. (2004). The gamma2 subunit of GABA(A) receptors is a substrate for palmitoylation by GODZ. J. Neurosci. *24*, 5881–5891.

Lane, S.R., and Liu, Y. (1997). Characterization of the palmitoylation domain of SNAP-25. J. Neurochem. *69*, 1864–1869.

Linder, M.E., and Deschenes, R.J. (2004). Model organisms lead the way to protein palmitoyltransferases. J. Cell Sci. *117*, 521–526.

Linder, M.E., Middleton, P., Hepler, J.R., Taussig, R., Gilman, A.G., and Mumby, S.M. (1993). Lipid modifications of G proteins: alpha subunits are palmitoylated. Proc. Natl. Acad. Sci. USA *90*, 3675–3679.

Lobo, S., Greentree, W.K., Linder, M.E., and Deschenes, R.J. (2002). Identification of a Ras palmitoyltransferase in Saccharomyces cerevisiae. J. Biol. Chem. *277*, 41268–41273.

Milligan, G., Parenti, M., and Magee, A.I. (1995). The dynamic role of palmitoylation in signal transduction. Trends Biochem. Sci. *20*, 181–187.

Mumby, S.M. (1997). Reversible palmitoylation of signaling proteins. Curr. Opin. Cell Biol. *9*, 148–154.

Oyama, T., Miyoshi, Y., Koyama, K., Nakagawa, H., Yamori, T., Ito, T., Matsuda, H., Arakawa, H., and Nakamura, Y. (2000). Isolation of a novel gene on 8p21.3–22 whose expression is reduced significantly in human colorectal cancers with liver metastasis. Genes Chromosomes Cancer *29*, 9–15.

Resh, M.D. (1999). Fatty acylation of proteins: new insights into membrane targeting of myristoylated and palmitoylated proteins. Biochim. Biophys. Acta *1451*, 1–16.

Robbins, S.M., Quintrell, N.A., and Bishop, J.M. (1995). Myristoylation and differential palmitoylation of the HCK protein-tyrosine kinases govern their attachment to membranes and association with caveolae. Mol. Cell. Biol. *15*, 3507–3515.

Ross, E.M. (1995). Protein modification. Palmitoylation in G-protein signaling pathways. Curr. Biol. *5*, 107–109.

Roth, A.F., Feng, Y., Chen, L., and Davis, N.G. (2002). The yeast DHHC cysteine-rich domain protein Akr1p is a palmitoyl transferase. J. Cell Biol. *159*, 23–28.

Shenoy-Scaria, A.M., Dietzen, D.J., Kwong, J., Link, D.C., and Lublin, D.M. (1994). Cysteine3 of Src family protein tyrosine kinase determines palmitoylation and localization in caveolae. J. Cell Biol. *126*, 353–363.

Singaraja, R.R., Hadano, S., Metzler, M., Givan, S., Wellington, C.L., Warby, S., Yanai, A., Gutekunst, C.A., Leavitt, B.R., Yi, H., et al. (2002). HIP14, a novel ankyrin domain-containing protein, links huntingtin to intracellular trafficking and endocytosis. Hum. Mol. Genet. *11*, 2815–2828.

Skene, J.H., and Virag, I. (1989). Posttranslational membrane attachment and dynamic fatty acylation of a neuronal growth cone protein, GAP-43. J. Cell Biol. *108*, 613–624.

Smotrys, J.E., and Linder, M.E. (2004). Palmitoylation of intracellular signaling proteins: Regulation and function. Annu. Rev. Biochem. *73*, 559–587.

Stein, V., House, D.R., Bredt, D.S., and Nicoll, R.A. (2003). Postsynaptic density-95 mimics and occludes hippocampal long-term potentiation and enhances long-term depression. J. Neurosci. *23*, 5503–5506.

Taylor, D.C., Weber, N., Hogge, L.R., and Underhill, E.W. (1990). A simple enzymatic method for the preparation of radiolabeled erucoyl-CoA and other long-chain fatty acyl-CoAs and their characterization by mass spectrometry. Anal. Biochem. *184*, 311–316.

Topinka, J.R., and Bredt, D.S. (1998). N-terminal palmitoylation of PSD-95 regulates association with cell membranes and interaction with K+ channel, Kv1.4. Neuron *20*, 125–134.

Uemura, T., Mori, H., and Mishina, M. (2002). Isolation and characterization of Golgi apparatus-specific GODZ with the DHHC zinc finger domain. Biochem. Biophys. Res. Commun. *296*, 492–496.

Vogel, K., and Roche, P.A. (1999). SNAP-23 and SNAP-25 are palmitoylated in vivo. Biochem. Biophys. Res. Commun. *258*, 407–410.

Wedegaertner, P.B., and Bourne, H.R. (1994). Activation and depalmitoylation of Gs alpha. Cell *77*, 1063–1070.

Wedegaertner, P.B., Chu, D.H., Wilson, P.T., Levis, M.J., and Bourne, H.R. (1993). Palmitoylation is required for signaling functions and membrane attachment of Gq alpha and Gs alpha. J. Biol. Chem. *268*, 25001–25008.

Zhao, L., Lobo, S., Dong, X., Ault, A.D., and Deschenes, R.J. (2002). Erf4p and Erf2p form an endoplasmic reticulum-associated complex involved in the plasma membrane localization of yeast Ras proteins. J. Biol. Chem. *277*, 49352–49359.